The Henryk Niewodniczański
INSTITUTE OF NUCLEAR PHYSICS
Polish Academy of Sciences
152 Radzikowskiego Str., 31-342 Kraków, Poland

www.ifj.edu.pl/reports/2005.html

Kraków, May 2005

Report No. 1962/D

Results obtained with the passive radiation detectors in the ICCHIBAN-4 experiment

Paweł Bilski, Tomasz Horwacik

Abstract

In frame of the InterComparison of Cosmic rays with Heavy Ions Beams at NIRS (ICCHIBAN) organized at the HIMAC accelerator in Chiba several types of the thermoluminescent detectors (TLD), as well as CR-39 track detectors, were exposed. Four different types of TLDs were used: MTS-7 (^{7}LiF:Mg,Ti), MTS-6 (^{6}LiF:Mg,Ti), MCP-7 (^{7}LiF:Mg,Cu,P) and MTT-7 (^{7}LiF:Mg,Ti with changed activator composition. All TLDs were manufactured at the Institute of Nuclear Physics (IFJ) in Krakow. The detectors were irradiated with various doses of He, C, Ne and Fe ions. Part of exposures were done in unknown conditions, to test measuring capabilities of the detectors. For analyses of these results, the method of obtaining information on ionisation density of an unknown radiation field, which is based on ratios of responses of different LiF detectors, was successfully used.

1. Introduction

Astronauts working in the Earth orbit are exposed to levels of cosmic radiation highly exceeding that received on the ground and space crews may be considered as most occupationally exposed profession. Many detector systems, both passive and active, have been used for measurements of radiation in space, but due to complexity of the radiation field interpretation of results in not always straightforward. Radiation field encountered in space contains a significant component of various high-energy ions. As detection efficiency of passive detectors depends on ionisation density, it is of importance to closely study the heavy ion response of detectors to be used in space dosimetry. Such an opportunity was created in frame of the ICCHIBAN project (InterComparison of Cosmic rays with Heavy Ions Beams at NIRS), organized at the HIMAC accelerator in Chiba. Results of the first run (ICCHIBAN-2) has been published elsewhere [Bilski & Horwacik 2004]. Present report describes results of the ICCHIBAN-4 phase of the project.

2. Detector

The detector set consisted of thermoluminescent detectors (TLDs) and CR-39 track detectors. Four different types of TLDs were used: MTS-7 (^{7}LiF:Mg,Ti), MTS-6 (^{6}LiF:Mg,Ti), MCP-7 (^{7}LiF:Mg,Cu,P) and MTT-7 (^{7}LiF:Mg,Ti with changed activator composition [Bilski 2004]). All TLDs were manufactured at the Institute of Nuclear Physics (IFJ) in Krakow, Poland. Their dimensions are: diameter 4.5 mm and thickness 0.6 mm. Following annealing conditions were applied for TLDs: for MTS and MTT: 400^{o}C/1h+100^{o}C/2h; for MCP-7 240^{o}C/10 minutes. MTS and MTT annealing were performed with the PTW TLDO automatic oven, with cooling of TLDs inside the oven. This is a difference with the procedure used within the previous phase - ICCHIBAN-2, when fast cooling with TLDs removed from the oven was applied. All TLDs were additionally annealed at 100^{o}C/10 min after exposure but prior to readout.

Calibration of TLDs (conversion of TL signal to gamma-ray dose) was done through irradiation of a group of TLDs of each type with 5 mGy (dose in water) of ^{137}Cs gamma-rays at the calibration facility of the IFJ. The dose rate of the source in terms of dose in water was obtained through calibration (with TLDs) against a ^{60}Co source in the Centre of Oncology in Krakow. Calibration exposure was done in the same time period as the ICCHIBAN irradiations to minimize any fading effects. Additionally, to correct spread of sensitivity between TLDs, the individual response factors for each detector were evaluated after the ICCHIBAN exposures.

CR-39 material of a trade name TASTRAK produced by the Track Analysis Systems, Bristol was applied for measurements. Detectors of dimensions 17 mm x 17 mm have been cut from 1.1 mm thick sheet and labeled. Before use all detectors were cleaned with ethanol.

For exposures detectors were mounted into polystyrene holders. Each holder contained 15 pcs of TLDs (5 pieces of each type) and a stack of three CR-39 detectors. The thickness of the polystyrene cover, which by the ion beam traverses before reaching the detectors, was 2 mm. Finally, the holders were sealed with aluminum foil.

3. Experiment and analysis

In total 26 detector packages were exposed with ions in frame of the ICCHIBAN-4. 18 packages were exposed as so called "known exposures", i.e within efficiency and linearity studies with known doses of He, C, Ne and Fe ions and 8 packages as so called "blind exposures" (i.e. with the unknown radiation field). The “known” exposures for each ion were done not only with the unmodulated beams, but also after crossing following preabsorbers: 5 g/cm^2 H_2O, 5 g/cm^2 Al and 10 g/cm^2 Al. The nominal absorbed dose for the exposures with the unmodulated beam was always 10 mGy. All irradiations were performed with the ion beam perpendicular to the package. Analyses of both used detector systems were done separately, i.e. results of track detectors were not used for any correction of TLD results, nor the other way round. Together with the exposed detectors, the organizers delivered to participants results of measurements of depth dose distribution in water for each ion. The estimation of actual energy and LET in water for all particles was performed by comparing the position of the Bragg peak of the measured dose distribution with the set of distributions calculated by SRIM2003.26 computer program [Ziegler & Biersack, 2003] (SRIM 2003 produces somewhat different results from the SRIM 2000 version, used previously for analysis of the ICCHIBAN-2). The values are presented in Table 1.

Table 1. Parameters of the ion beams used during the ICCHIBAN-2.

Ion	Nominal energy, MeV/n	Estimated energy, MeV/n	Estimated LET, keV/μm
^{4}He	150	144	2.26
^{12}C	400	380	11.0
^{20}Ne	400	365	31.5
^{56}Fe	500	412	199.3

With the TRIM Monte Carlo program, which is a part of the SRIM2003 package, it is possible to estimate energy of ions transmitted through an absorbing layer. In this way the water equivalents of

the applied aluminum layers were found. Then, exploiting the depth-dose data for water (given by organizers) it was possible to estimate doses delivered to detectors at different depths. Results of these calculations are given in Table 2. It should be however pointed out that values of dose (and LET) obtained in that way are certainly biased with larger uncertainties than those known for the primary ion beams. The thickness of 10 g/cm^2 Al is just beyond the Bragg peak position for 412.1 MeV/u Fe ions, so assessment of dose and LET was in this case not possible.

Table 2. Estimated parameters of ion beams after crossing the absorbing layers.

Ion		E, MeV/u	LET, keV/μm	D, mGy
He	5g/cm^2 Al= 3.9 g/cm^2 H_2O	120.3	2.57	10.88
	5g/cm^2 H_2O	113.0	2.69	11.22
	10g/cm^2 Al= 7.75 g/cm^2 H_2O	93.3	3.10	12.41
C	5g/cm^2 Al= 3.9 g/cm^2 H_2O	343.3	11.60	9.52
	5g/cm^2 H_2O	332.5	11.75	9.54
	10g/cm^2 Al= 7.75 g/cm^2 H_2O	304.8	12.83	9.73
Ne	5g/cm^2 Al= 3.9 g/cm^2 H_2O	300.2	34.92	9.7
	5g/cm^2 H_2O	280.8	36.31	9.7
	10g/cm^2 Al= 7.75 g/cm^2 H_2O	227.6	41.30	9.9
Fe	5g/cm^2 Al= 3.9 g/cm^2 H_2O	256.2	256.9	10.90
	5g/cm^2 H_2O	202.0	297.7	11.96

TL measurements were carried out with the RA'94 manual reader (manufactured by the Mikrolab Krakow) equipped with platinum planchet heating system, a PM tube with a bialkali photocathode and BG-12 filter. The heating rate was 10^{o}C/s. Figure 2 illustrates examples of the measured glow-curves. For MTS-7, MTS-6 and MTT-7 glow-curves were integrated in two separate regions, called further main peak integral and high-temperature peak integral. Separation between these two peaks is shown in figure 1. Further analyses were based mostly on the main peak integrals. For MCP-7 integral of the whole glow-curve was taken.

For each measurement an average of the 5 TLDs was calculated. From these results the TL signals of transport background detectors were subtracted.

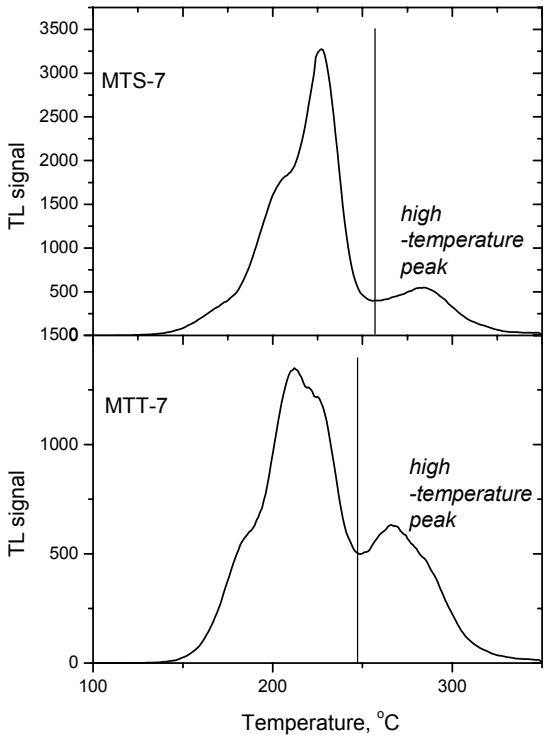

Figure 1. Examples of MTS-7 and MTT-7 glow-curves and separation between high-temperature and main peak.

For track analysis one CR-39 detector (from three in the stack) were etched. Remaining two detectors have been sealed again and kept in case of an etch failure. All chosen detectors were etched together for 20 hours in 7 N water solution of NaOH at the temperature of 70^{O} C. The thickness of removed layer has been found to be on average 37 μm (from one side of a detector) and the corresponding bulk etch rate was 1.84 μm/hour. Effective area of the detector (available for readout) was about 2 cm^2 after etching. The PZO StudarLAB optical microscope with manual control stage and the OSCAR CCD camera were used for readout. Track parameters were measured with the use of the UTHSCSA *ImageTool* program (developed at the University of Texas Health Science Center at San Antonio, Texas). Range of magnifications used during readout varied between 100 and 400. The measured quantities were the diameter of the track and the number of tracks per unit detector surface (track density). Formula (1) was used to determine track etch rate [Durrani & Bull, 1987].

$$V_T = V_B \frac{4V_B^2 t^2 + d^2}{4V_B^2 t^2 - d^2} \tag{1}$$

where: t - time of etching, V_T - track etch rate, V_B – bulk etch rate, d – diameter of the track.

The scanning of the surface of each detector was done manually. At least 100 tracks of each type have been measured in order to obtain the distribution of V_T/V_B ratio. The Gauss curve was then fitted to this distribution and the values of it's maximum and width were used in further calculations. V_T/V_B

ratio has been determined for all types of tracks from known exposures except for ^{4}He ions and for ^{56}Fe ions passing through 10 g/cm^2 layer of Al (see Table 6). Tracks of 2.26 keV/μm helium ions were not registered in CR-39. However tracks of secondary particles resulting from nuclear reactions were observed and their number was increasing with fluence.

Values of dose and dose equivalent for blind exposures have been found with the use of following formulas:

$$D = \frac{1.602 \times 10^{-6}}{\rho_{H_2O}} \sum_i f(i) * LET(i) \quad [mGy] \tag{2}$$

$$H = \frac{1.602 \times 10^{-6}}{\rho_{H_2O}} \sum_i f(i) * Q(i) * LET(i) \quad [mSv] \tag{3}$$

where: ρ_{H2O} - density of water, f(i)-fluence of the particle with LET(i), Q(i)- the LET dependent Quality Factor [ICRP 1991].

Values of mean quality factor have been found with the use of formula:

$$\overline{Q} = \frac{\sum_i Q(i) * D(i)}{D} \tag{4}$$

where: Q(i) – LET dependent quality factor for each type of particle, D(i) – absorbed dose due to each type of particle, D – total absorbed dose

4. Results

4.1 Known exposures

4.1.1 Thermoluminescent detectors

Table 3 presents doses measured with all TLD types and for all radiation modalities (using Cs-137 calibration). The differences in efficiency between MTT, MTS and MCP known from earlier measurements are apparent. It can be noticed that MTS-6 detectors show usually slightly higher doses than MTS-7. This is however probably due to uncertainties of measurements, rather than due to the presence of neutrons. MTS-6 results are not used for further analysis.

Table 3. The doses in mGy measured with four TLD types for all radiation modalities during the known exposures (using Cs-137 calibration).

	MTS-7	MTT-7	MCP-7	MTS-6
He	10.4±0.2	11.0±0.5	7.7±0.1	10.8±0.1
He 5 g/cm^2 Al	11.9±0.1	12.4±0.8	8.5±0.5	11.9±0.1
He 10 g/cm^2 Al	13.4±0.2	13.5±0.4	9.1±0.1	13.5±0.3
He 5 g/cm^2 H_20	12.0±0.2	12.0±0.5	8.5±0.1	12.2±0.1
Ne 10 mGy	6.1±0.1	8.1±0.3	3.7±0.1	6.4±0.1
Ne 50 mGy	30.3±0.7	42.2±1.3	18.8±0.7	31.1±0.4
Ne 100 mGy	60.8±0.3	82.0±3.1	36.6±1.1	63.4±0.2
Ne 5 g/cm^2 Al	6.0±0.2	8.0±0.4	3.7±0.1	6.4±0.2
Ne 10 g/cm^2 Al	6.3±0.1	8.1±0.4	3.8±0.1	6.6±0.2
Ne 5 g/cm^2 H_20	5.9±0.2	8.0±0.4	3.5±0.1	6.1±0.1
C	8.9±0.2	10.2±0.5	5.3±0.2	9.3±0.1
C 5 g/cm^2 Al.	8.8±0.2	9.9±0.2	5.7±0.1	9.1±0.1
C 10 g/cm^2 Al	8.7±0.1	9.5±0.2	5.0±0.3	8.6±0.2
C 5 g/cm^2 H_20	8.1±0.3	9.1±0.3	4.7±0.1	8.3±0.1
Fe	4.3±0.2	5.9±0.2	3.0±0.1	4.3±0.1
Fe 5 g/cm^2 Al	4.8±0.1	6.9±0.6	3.2±0.1	5.1±0.1
Fe 10 g/cm^2 Al	0.79±0.04	1.09±0.10	0.48±0.01	0.71±0.04
Fe 5 g/cm^2 H_20	5.0±0.1	7.3±0.6	3.3±0.1	5.2±0.1

Figures 2-4 presents relative efficiency η of TLDs in function of LET. The current results are compared with those obtained within the ICCHIBAN-2 and additionally with results measured at the Dubna proton beam (155 MeV) using TLDs from exactly the same batches. Solid lines represent the fitted empirical functions: MTS-7 and MTT-7 according to equation (5) and MCP-7 according to equation (6). The fitted parameters are given in Table 4.

$$\eta = a\exp(-bx) + c \tag{5}$$

$$\eta = a\exp(-bx) + c + \frac{d}{1+fx} \tag{6}$$

Table 4.
Parameters of the fitted equations

Parameter	MTS-7	MTT-7	MCP-7
a	0.603	0.511	0.232
b	0.032	0.020	0.063
c	0.446	0.579	0.283
d	-	-	0.474
f	-	-	0.268

The choice of the fitted models is purely empirical and in general it is probably incorrect, as TL efficiency is not necessary a unique function of LET [Geiss, 1998; Olko, 2002]. The most apparent observation is that results of the ICCHIBAN-2 and ICCHIBAN-4 agree very well. This is an important information, which means that the mentioned change of annealing procedure for LiF:Mg,Ti detectors (slow cooling down after 400^{o}C) has no significant influence on the relative efficiency.

All LiF:Mg,Ti detectors consequently show efficiency exceeding unity for He ions. It is interesting that no such effect is observed for the proton irradiations performed in Dubna.

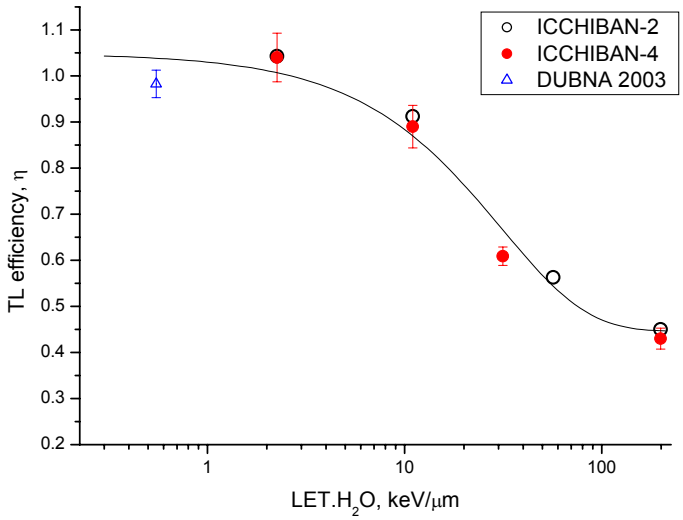

Figure 2. Relative efficiency of MTS-7 detectors vs LET. Detailed description in the text.

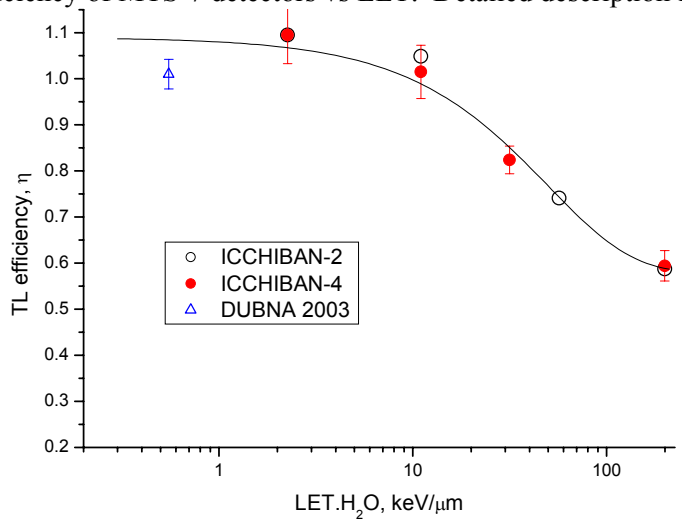

Figure 3. Relative efficiency of MTT-7 detectors vs LET. Detailed description in the text.

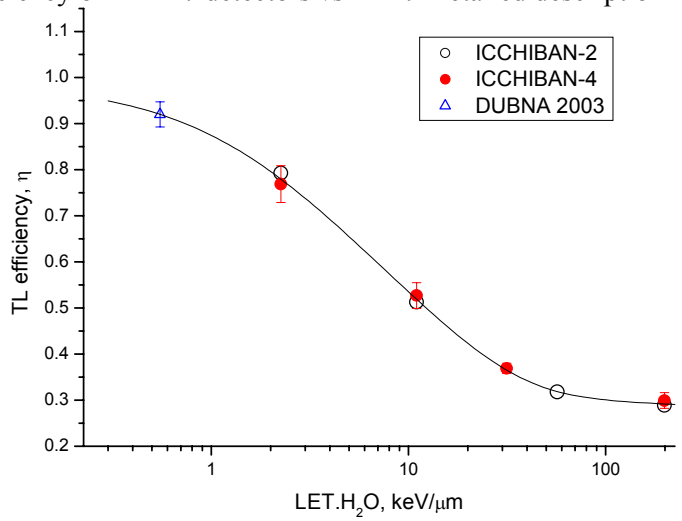

Figure 4. Relative efficiency of MCP-7 detectors vs LET. Detailed description in the text.

Figure 5 presents results of the dose linearity study for Ne ion (this exposure was a supplement to the linearity tests performed for other ions during the ICCHIBAN-2) in terms of TL efficiency (dose measured/dose delivered). It can be seen that the efficiency of all used TLD types does not depend on dose within the tested dose range.

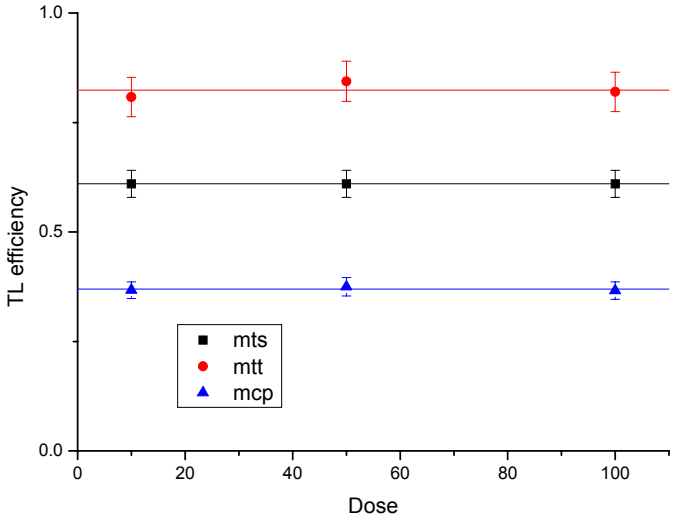

Figure 5. Relative TL efficiency (dose measured divided by dose delivered) for Ne ions. Solid lines represent average efficiency.

Table 5. Ratios of the integrals of high-temperature/main peak for three LiF:Mg,Ti detector types for all radiation modalities.

	MTS-7	MTT-7	MTS-6
He	0.13±0.005	0.13±0.06	0.18±0.01
He 5 g/cm^2 Al	0.12±0.006	0.18±0.06	0.20±0.004
He 10 g/cm^2 Al	0.13±0.007	0.27±0.01	0.22±0.01
He 5 g/cm^2 H_20	0.12±0.005	0.24±0.02	0.20±0.01
Ne 10 mGy	0.52±0.02	0.89±0.04	0.69±0.01
Ne 50 mGy	0.50±0.02	0.89±0.05	0.70±0.03
Ne 100 mGy	0.52±0.01	0.96±0.05	0.70±0.02
Ne 5 g/cm^2 Al	0.54±0.02	0.85±0.05	0.69±0.02
Ne 10 g/cm^2 Al	0.52±0.02	0.89±0.06	0.69±0.03
Ne 5 g/cm^2 H_20	0.52±0.02	0.85±0.06	0.68±0.01
C	0.29±0.01	0.53±0.04	0.41±0.01
C 5 g/cm^2 Al.	0.28±0.02	0.51±0.04	0.40±0.01
C 10 g/cm^2 Al	0.29±0.008	0.54±0.02	0.43±0.02
C 5 g/cm^2 H_20	0.29±0.01	0.54±0.04	0.41±0.01
Fe	0.55±0.03	1.04±0.06	0.49±0.03
Fe 5 g/cm^2 Al	0.55±0.03	0.99±0.10	0.77±0.02
Fe 10 g/cm^2 Al	0.60±0.07	0.93±0.13	0.95±0.07
Fe 5 g/cm^2 H_20	0.55±0.03	1.02±0.10	0.77±0.01

It is a well known property of LiF:Mg,Ti TL materials that the high-temperature peaks of the glow curve show stronger response to high-LET radiation than the main peak. To study this effect, the ratio of integrals of both peaks: the high-temperature to the main was calculated. The results are presented

in Table 5. In Figure 6 peak ratios measured during the ICCHIBAN-4 are compared with those obtained during the ICCHIBAN-2. The apparent difference in the peak ratio values is an effect of the slow cooling rate after annealing applied in the present experiment.

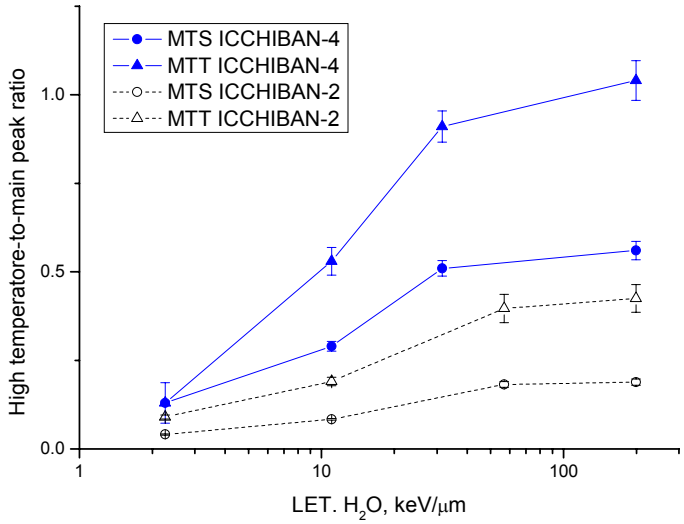

Figure 6. Ratios of high-temperature to main peak integrals vs. LET.

4.1.2 CR-39 track detectors

The values of the V_T/V_B ratio calculated after known exposures are presented in Table 6. It may be noticed, that there are only slight differences between results obtained for detectors irradiated with ^{12}C ions. The value of V for ^{20}Ne ions passing through 5 g/cm^2 layer of H_2O was found to be significantly lower than expected and this point has been excluded from the calibration curve.

Table 6. Calculated values of V_T/V_B ratio for ^{12}C, ^{20}Ne and ^{56}Fe ions.

Ion type and shielding	$V=V_T/V_B$
^{12}C mono	1.034 ± 0.02
^{12}C 5 g/cm^2 H_2O	1.034 ± 0.02
^{12}C 5 g/cm^2 Al	1.042 ± 0.02
^{12}C 10 g/cm^2 Al	1.043 ± 0.02
^{20}Ne 5 mono	1.25 ± 0.02
^{20}Ne 5 g/cm^2 H_2O	1.18 ± 0.02
^{20}Ne 5 g/cm^2 Al	1.31 ± 0.02
^{20}Ne 10 g/cm^2 Al	1.37 ± 0.04
^{56}Fe mono	2.39 ± 0.04
^{56}Fe 5 g/cm^2 H_2O	2.98 ± 0.07
^{56}Fe 5 g/cm^2 Al	2.86 ± 0.07
^{56}Fe 10 g/cm^2 Al	-

The calibration curve LET_{H2O} vs. V-1 (see Figure 7) was established by fitting a polynomial (LET_{H2O} is in keV/μm, V is dimensionless):

$$LET_{H2O} = 7.55 + 86.46 *(V-1) + 34.90*(V-1)^2$$

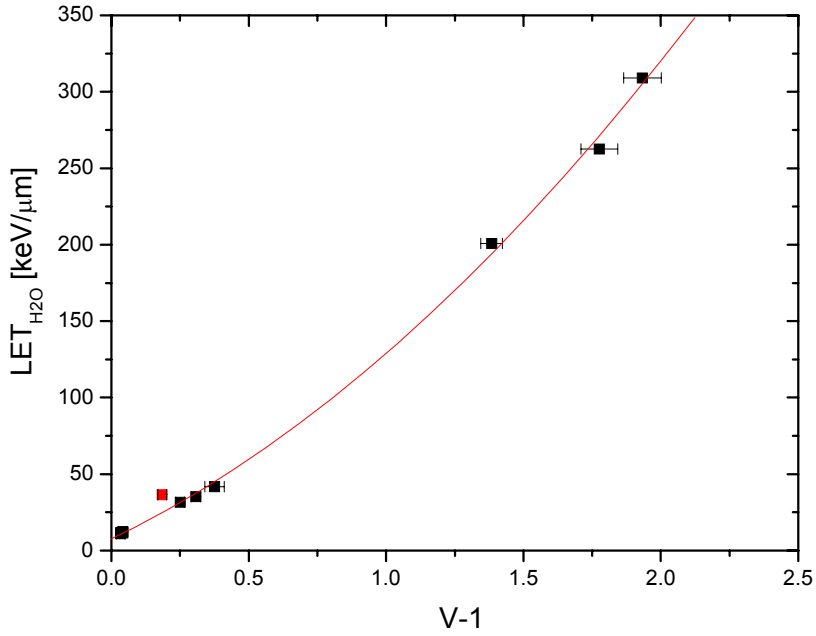

Figure 7. Dependence of V-1 ratio on ion's LET in water.

Linearity of the CR–39 detector dose response to ^{20}Ne ion is presented in Table 7. At high doses, tracks on the detector's surface overleaped and tips of the tracks had to be counted.

Table 7. Linearity of the CR-39 response to ^{20}Ne ions.

^{20}Ne	10 [mGy]	50 [mGy]	100 [mGy]
Fluence measured [1/cm^2]	185575 ± 8876	795166 ± 53355	1583327 ±74473
Response [tracks*mGy^{-1}*cm^{-2}]	18557 ± 888	15903±1067	15833 ± 744

4.2 Blind exposures

4.2.1 Thermoluminescent detectors

In Table 8 are presented results obtained directly after calibration with gamma rays, without introducing any corrections. Applying of such corrections is possible when ratio of responses of different detector types or high-temperature peak ratio are considered.

Table 8. Uncorrected values of doses (only Cs-137 calibration) measured with TLDs for the blind exposures.

	MTS-7 mGy	MTT-7 mGy	MCP-7 mGy
Blind 1	28.10±0.50	26.74±0.19	28.00±0.59
Blind 2	29.65±0.46	28.64±0.76	27.85±0.37
Blind 3	26.70±0.26	25.64±0.56	19.46±0.40
Blind 4	12.50±0.26	12.64±0.51	11.91±0.10
Blind 5	7.93±0.11	8.94±0.36	5.89±0.19
Blind 6	0.15±0.03	0.19±0.04	0.10±0.01
Blind 7	0.44±0.03	0.63±0.14	0.28±0.01
Blind 8	21.56±0.39	25.31±0.71	12.32±0.28

Figure 8-10 show response ratios of the used TLD types vs. LET. Ratios measured for the blind exposures are also plotted against the "guessed" values of LET. Solid lines represent the calculated ratio of the fitted functions (according to eq. 5 and 6). For blind exposures 1,2 and 4 response of all TLD types were similar. The response ratios for these exposures were usually even lower than those corresponding to high-energy proton irradiations. This may suggest that these detector packages were exposed with weakly ionizing radiation like gamma-rays or electrons and consequently no corrections were applied to the measured doses. For other blind exposures an approximate agreement with the general trend can be usually achieved not only for a single value of LET, but for some ranges of LET values – particularly for the lowest doses (Blind 6 and 7) the uncertainties of LET estimation are very high. For these LET ranges the relative efficiencies of each TLD type were then calculated (using eq. 5 and 6). The averages of obtained in this way values of efficiency were then used to correct the measured doses. The results are presented in Table 10.

A similar analysis can be also performed using ratios of the integrals of high-temperature/main peak for two LiF:Mg,Ti detector types. These ratios are presented in Table 9 and in figure 11. However peak ratios were not exploited for correcting the measured doses, due to two reasons: very high uncertainties at low doses (high-temperature peak is overlapped with the background signal) and limited number of available calibration data (as mentioned above applying somewhat different annealing procedure changed significantly intensity of the high-temperature peak).

For MCP-7 detectors one more approach was possible. It was found that MCP-7 relative efficiency can be directly connected to the TLDs response ratio. This is illustrated in figures 12-14. In this way it is possible to establish a correction of MCP efficiency without estimation of the LET value. The results of this approach are given in Table 10 under the name "method 2". For MTS and MTT such approach was not possible, because their efficiency does not decrease so steeply with LET, as in case of MCP, and consequently the trend is covered by spread of the data points.

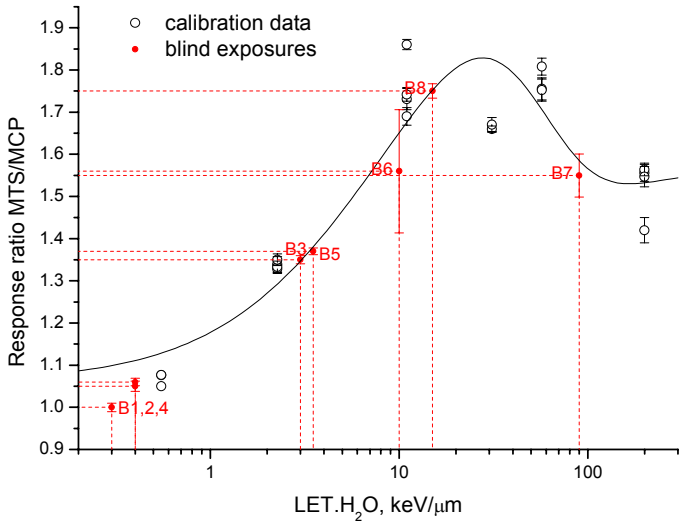

Figure 8. MTS/MCP response ratio. Data points represent all calibration results of the ICCHIBAN-2 and -4 ("known" exposures) and proton exposures at Dubna obtained for different doses. Solid line represents the calculated ratio of the fitted functions (eq. 5 and 6). Values of LET for the blind exposures were guessed in this way that the measured data approximately fit to the calculated function.

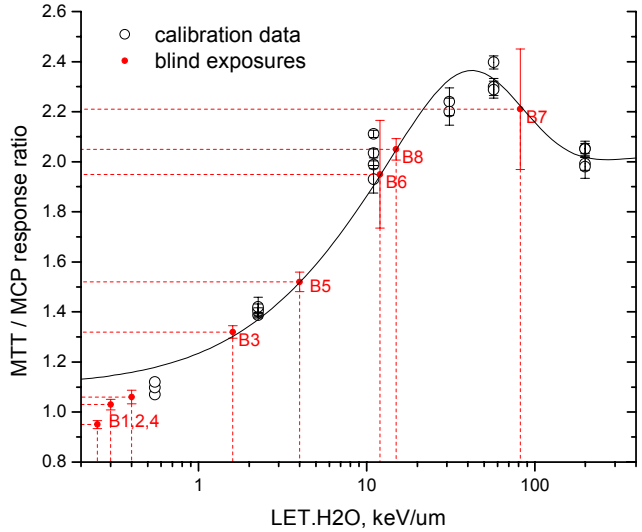

Figure 9. MTT/MCP response ratio. Data points represent all calibration results of the ICCHIBAN-2 and -4 ("known" exposures) and proton exposures at Dubna obtained for different doses. Solid line represents the calculated ratio of the fitted functions (eq. 5 and 6). Values of LET for the blind exposures were guessed in this way that the measured data approximately fit to the calculated function.

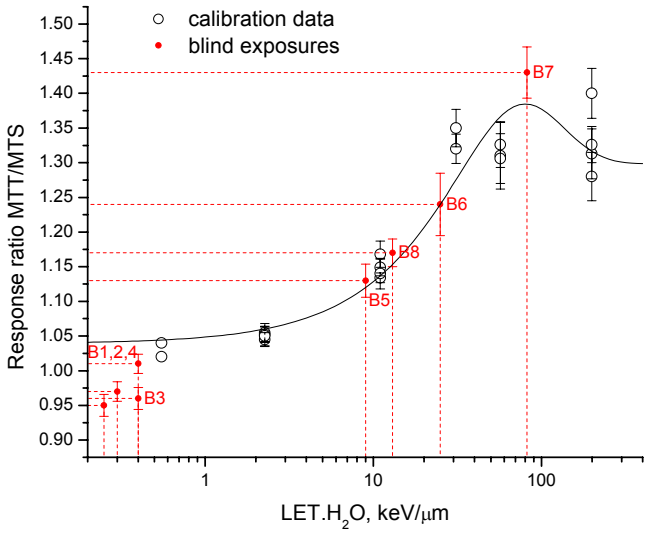

Figure 10 MTT/MTS response ratio. Data points represent all calibration results of the ICCHIBAN-2 and -4 ("known" exposures) and proton exposures at Dubna obtained for different doses. Solid line represents the calculated ratio of the fitted functions (eq. 5). Values of LET for the blind exposures were guessed in this way that the measured data approximately fit to the calculated function.

Table 9. Ratios of the integrals of high-temperature/main peak for two LiF:Mg,Ti detector types for the blind exposures.

	MTS-7	MTT-7
Blind 1	0.08±0.002	0.18±0.008
Blind 2	0.08±0.003	0.18±0.010
Blind 3	0.11±0.008	0.24±0.015
Blind 4	0.08±0.003	0.11±0.038
Blind 5	0.24±0.011	0.45±0.030
Blind 6	0.72±0.270	0.25±0.431
Blind 7	0.60±0.060	0.65±0.293
Blind 8	0.28±0.012	0.51±0.020

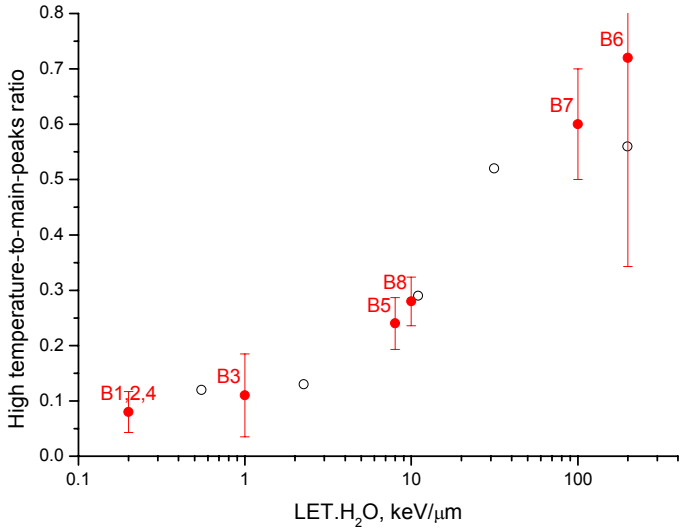

Figure 11. Ratios of high-temperature to main peak integrals vs. LET for MTS-7 TLDs. Values of LET for the blind exposures were guessed in this way that the measured data approximately fit to the trend.

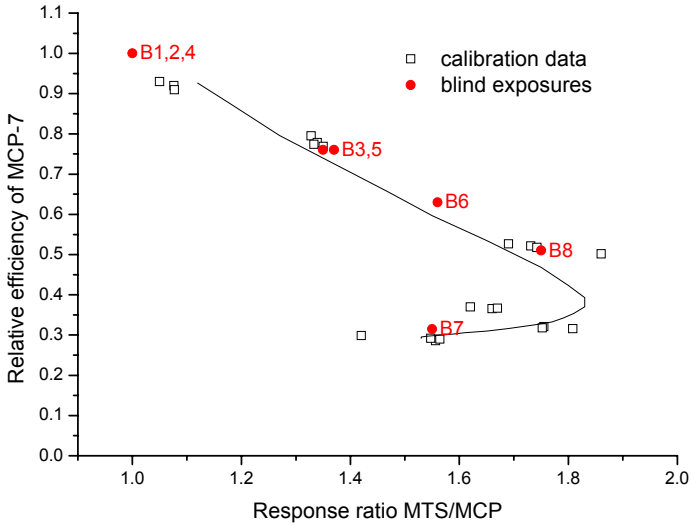

Figure 12. Relative efficiency for MCP-7 vs. MTS/MCP response ratio. Solid line represents the values calculated using the fitted previously functions (eq. 5 and 6). Values of efficiency for the blind exposures were guessed in this way that the measured data approximately fit to the trend.

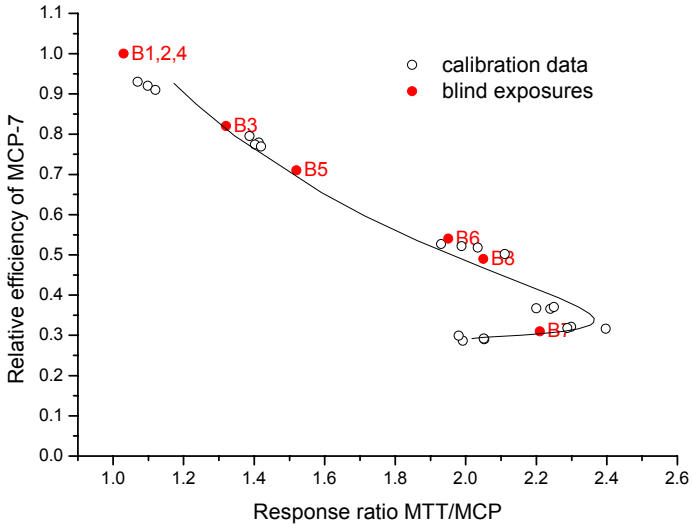

Figure 13. Relative efficiency for MCP-7 vs. MTT/MCP response ratio. Solid line represents the values calculated using the fitted previously functions (eq. 5 and 6). Values of efficiency for the blind exposures were guessed in this way that the measured data approximately fit to the trend.

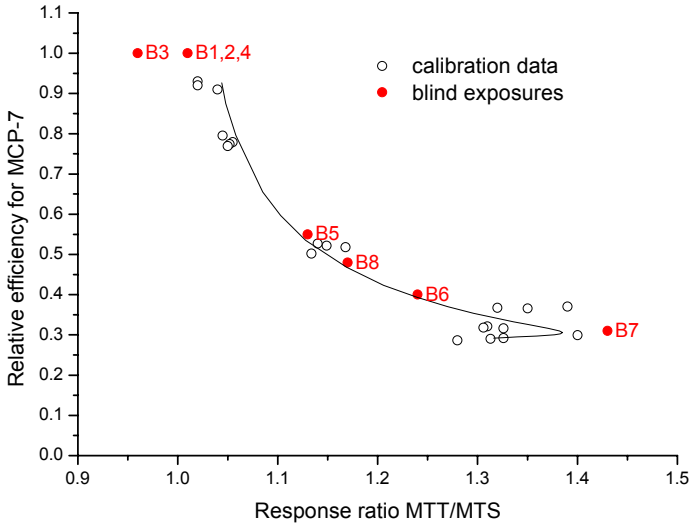

Figure 14. Relative efficiency for MCP-7 vs. MTT/MTS response ratio. Solid line represents the values calculated using the fitted previously functions (eq. 5 and 6). Values of efficiency for the blind exposures were guessed in this way that the measured data approximately fit to the trend.

Table 10. The final corrected values of doses measured with TLDs for the blind exposures. For MCP detectors two methods of correction were applied: method 1, which is identical with that used for MTS and MTT, and method 2. The detailed description in the text.

	MTS-7 [mGy]	MTT-7 [mGy]	MCP-7 [mGy]	
			method 1	method 2
Blind 1*	28.10±0.50	26.74±0.19	28.00±0.59	
Blind 2*	29.65±0.46	28.64±0.76	27.85±0.37	
Blind 3	26.4±0.4	24.0±0.2	24.4±1.6	24.6±1.7
Blind 4*	12.50±0.26	12.64±0.51	11.91±0.10	
Blind 5	8.1±0.1	8.5±0.1	8.4±0.3	8.0±0.1
Blind 6	0.26±0.08	0.25±0.06	0.29±0.07	0.33±0.02
Blind 7	0.83±0.22	0.87±0.18	0.88±0.20	0.85±0.17
Blind 8	25.6±1.4	26.0±0.8	25.1±2.4	24.3±1.0

(*) – no correction was applied for blind exposures 1, 2 and 4.

4.1.2 CR-39 track detectors

The results of blind exposures of track detectors are presented below. In each case the number of counted tracks was corrected for registration efficiency. An additional correction was applied in case of ^{12}C ions which are very small and are easily covered by much larger tracks. In this correction a real area available for track counting was measured and then the density of ^{12}C ions tracks was recalculated.

Blind 1 and Blind 2

Only tracks originated from background exposure appeared on the surfaces of detectors from Blind 1 and Blind 2 exposures (see Figure 15). The lack of other tracks suggests, that they were irradiated with particles, which are not able to produce tracks in CR–39 material.

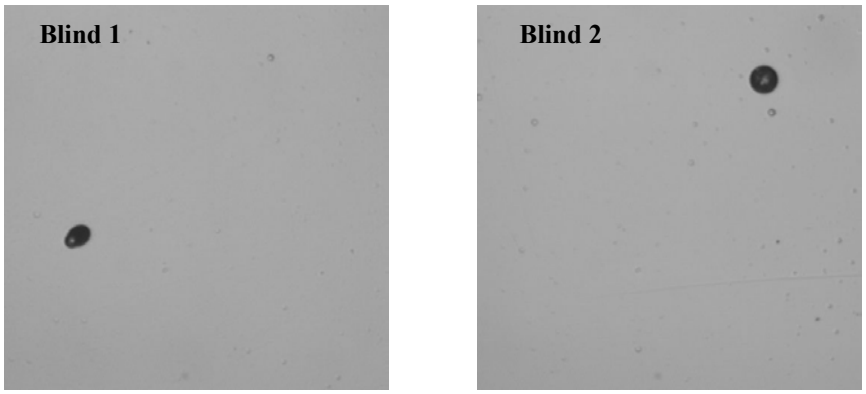

Figure 15. Background tracks on the surfaces of detectors from Blind 1 and Blind 2 irradiations (magn. 100x).

Blind 3

There is a significant number of tracks on both sides of the detector. Comparison of the upper and lower surfaces of the detector indicates, that there is no symmetry between them (see Figure 16). It could mean that this detector was irradiated with ^{4}He ions of unknown fluence.

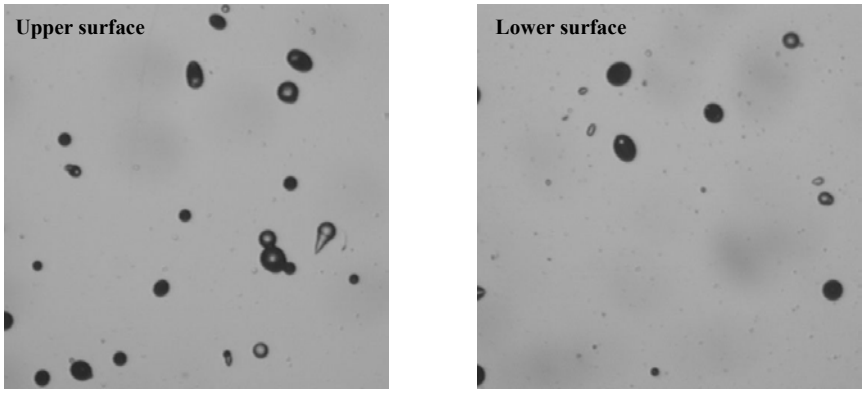

Figure 16. Tracks of secondary particles on the surface of detector from Blind 3 irradiation (magn. 100x).

Blind 4

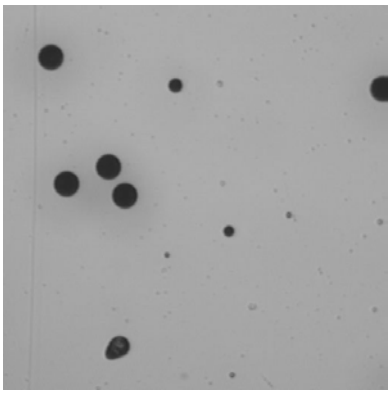

Figure 17. Tracks of ^{12}C, ^{20}Ne and ^{56}Fe ions on the surface of detector from Blind 4 irradiation (magn. 100x).

Table 11. CR-39 results of blind 4 irradiation

Blind 4	^{12}C	^{20}Ne	^{56}Fe	Total or Average
Fluence [1/cm^2]	1268 ± 92	568 ± 52	1065 ± 70	2902 ± 126
LET H_2O [keV/um]	10.8 ± 1.0	34.7 ± 2.4	189.8 ± 13.5	
D corr [mGy]	0.02 ± 0.01	0.03 ± 0.01	0.32 ± 0.05	0.38±0.06
Q	1.3	8.9	21.8	19.5 ± 2.0
H [mSv]	0.028 ± 0.01	0.28 ± 0.05	7.05 ± 1.0	7.36 ± 1.0

Blind 5

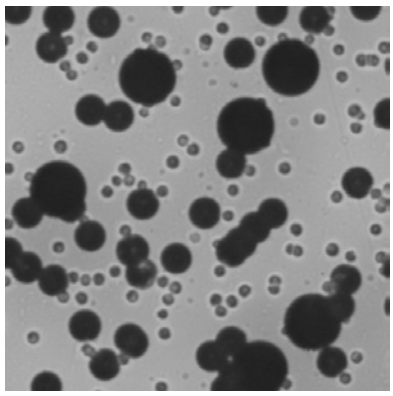

Figure 17. Tracks of ^{12}C, ^{20}Ne and ^{56}Fe ions on the surface of detector from Blind 5 irradiation (magn. 200x)

Table 12. CR-39 results of blind 5 irradiation

Blind 5	^{12}C	^{20}Ne	^{56}Fe	Total or Average
Fluence [1/cm^2]	$(11.1 \pm 0.16)\cdot 10^4$	$(3.6 \pm 0.02)\cdot 10^4$	$(0.65 \pm 0.01)\cdot 10^4$	$(15.3 \pm 0.16)\cdot 10^4$
LET H_2O [keV/um]	11.1 ± 1.0	35.6 ± 3.2	197.9 ± 17.5	
D corr [mGy]	1.97 ± 0.34	2.04 ± 0.37	2.08 ± 0.37	6.10±0.6
Q	1.3	9.2	21.3	10.8 ± 1.8
H [mSv]	2.66 ± 0.46	18.70 ± 3.40	44.27 ± 7.92	65.6 ± 8.6

Blind 6

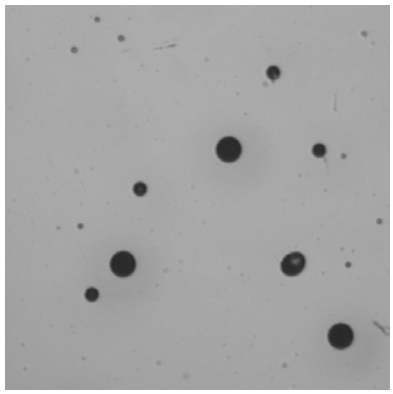

Figure 18. Tracks of ^{12}C, ^{20}Ne and ^{56}Fe ions on the surface of detector from Blind 6 irradiation (magn. 100x)

Table 13. CR-39 results of blind 6 irradiation

Blind 6	^{12}C	^{20}Ne	^{56}Fe	Total or Average
Fluence [1/cm^2]	1222 ± 70	676 ± 32	965 ± 46	2863 ± 120
LET H_2O [keV/um]	11.2 ± 1.5	35.5 ± 3.9	188.4 ± 10.7	
D corr [mGy]	0.022 ± 0.004	0.04 ± 0.004	0.29 ± 0.05	0.35±0.04
Q	1.4	9.2	21.9	19.2 ± 1.8
H [mSv]	0.030 ± 0.006	0.35 ± 0.04	6.37 ± 0.47	6.75 ± 1.60

Blind 7

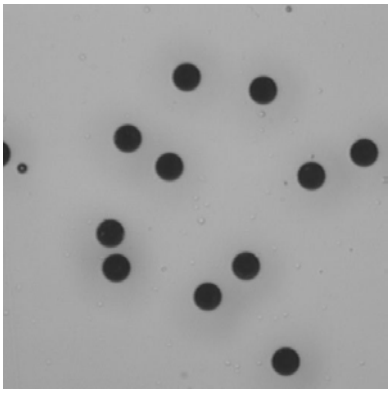

Figure 19. Tracks of ^{56}Fe ions on the surface of detector from Blind 7 irradiation (magn. 100x).

Table 14. CR-39 results of blind 7 irradiation

Blind 7	^{56}Fe	Total or Average
Fluence [1/cm^2]	2939 ± 134	2939 ± 134
LET H_2O [keV/um]	259.6 ± 27.2	259.6 ± 27.2
D corr [mGy]	1.22 ± 0.26	1.22 ± 0.26
Q	18.6	18.6
H [mSv]	22.75 ± 2.44	22.75 ± 2.44

Blind 8

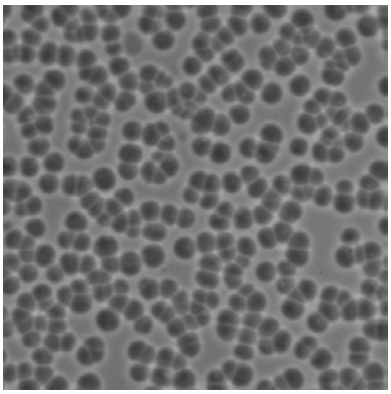

Figure 20. Tracks of ^{12}C ions on the surface of detector from Blind 8 irradiation (magn. 400x)

Table 15. CR-39 results of blind 8 irradiation

Blind 8	^{12}C	Total or Average
Fluence [1/cm^2]	$(15.0 \pm 0.15)\cdot 10^5$	$(15.0 \pm 0.15)\cdot 10^5$
LET H_2O [keV/um]	10.5 ± 0.6	10.5 ± 0.6
D corr [mGy]	25.2 ± 2.8	25.2 ± 2.8
Q	1.2	1.2
H [mSv]	29.04 ± 3.2	29.04 ± 3.2

5. Conclusions

In general all TLDs exhibited similar values of relative efficiency as in the ICCHIBAN-2 experiment. This quite good agreement was observed in spite of different annealing procedure applied for LiF:Mg,Ti detectors within the ICCHIBAN-4 (slower cooling rate). While the annealing conditions seem to have no significant influence on relative efficiency of the main dosimetric peak, the intensity of the high-temperature peaks was strongly changed.
Relative efficiency of both types of LiF:Mg,Ti detectors was again found to exceed unity for He ions. It is interesting that such effect was not observed for the 155 MeV proton irradiations performed in Dubna with the same TLDs. While this overresponse is small, it seems to be higher than statistical uncertainties of TL measurements. To be certain if this is a real effect further studies and careful check of gamma and/or ion dose calibration are needed.

For the blind exposures, the method of obtaining information on ionization density of an unknown radiation field, which is based on ratios of responses of different LiF detectors, was used. It seems that it can be successfully applied for correcting the measured doses for decreased TL efficiency. This method requires considerable further work on collecting more experimental data of the TL efficiency of three LiF TLDs for various radiation fields and obtaining mathematical description of the relationship between the TL efficiency and ionization density.

The response of CR-39 track detectors to ^{20}Ne appeared to be linear. Tracks of He ions were not registered, however secondary particles originated by these ions were observed. The registration efficiency of ^{12} C ions in mixed ion fields could be improved by measuring the real area available for track counting. However this method works correctly only at low fluences of other ions, when ^{12}C track are not totally covered by bigger tracks such as tracks of ^{56}Fe ions.

The ICCHIBAN-4 project resulted in gaining a considerable experimental data, which will enable further improvement of measuring techniques. This experience will be exploited in application of passive detectors in radiation measurements in space.

Acknowledgments

This experiment was performed as part of the ICCHIBAN research project using Heavy Ions at NIRS-HIMAC. This work was also partly supported by a research project from the Polish State Committee of Scientific Research (KBN) over the years 2003-2005 (No. 4T10C 038 24).

References

[Bilski & Horwacik] Bilski, P. and Horwacik, T. (2004) „Results obtained with the INP Kraków passive detectors in the ICCHIBAN-6 experiment" in "Results of the first two InterComparison of dosimetric instruments for Cosmic radiation with Heavy Ions at NIRS" HIMAC-078, eds. Y. Uchihori and E.R. Benton

[Bilski et al., 2004] Bilski, P., Budzanowski, M., Olko, P., Mandowska, E. (2004) " LiF:Mg,Ti (MTT) TL detectors optimised for high-LET radiation dosimetry", *Radiat. Meas.* 38, 427-430

[Durrani & Bull, 1987] Durrani, S.A., Bull, R.K. (1987) "Solid State Nuclear Track Detection Principles, Methods and Application" Pergamon Press

[Geiss et al., 1998] Geiss, O.B., Kramer, M., Kraft, G. (1998) "Efficiency of thermoluminescent detectors to heavy charged particles", *Nucl. Instr. Meth. B* **142** 592-598.

[ICRU, 1991] International Commission on Radiological Protection (1991). "1990 Recommendations of the International Commission on Radiological Protection". Pergammon Oxford, UK

[Olko et al., 2002] Olko, P., Bilski, P., Budzanowski, M., Waligórski, M.P.R. and Reitz, G. (2002) "Modeling the Response of Thermoluminescent Detectors Exposed to Low- and High-LET Radiation Fields*", J. Radiat. Res*., **43**: SUPPL., S59-S62

[Ziegler & Biersack, 2003] Ziegler, J.F., Biersack, J.P., "The Stopping and Range of Ions in Matter - SRIM 2003". www.srim.org